

Supporting Information

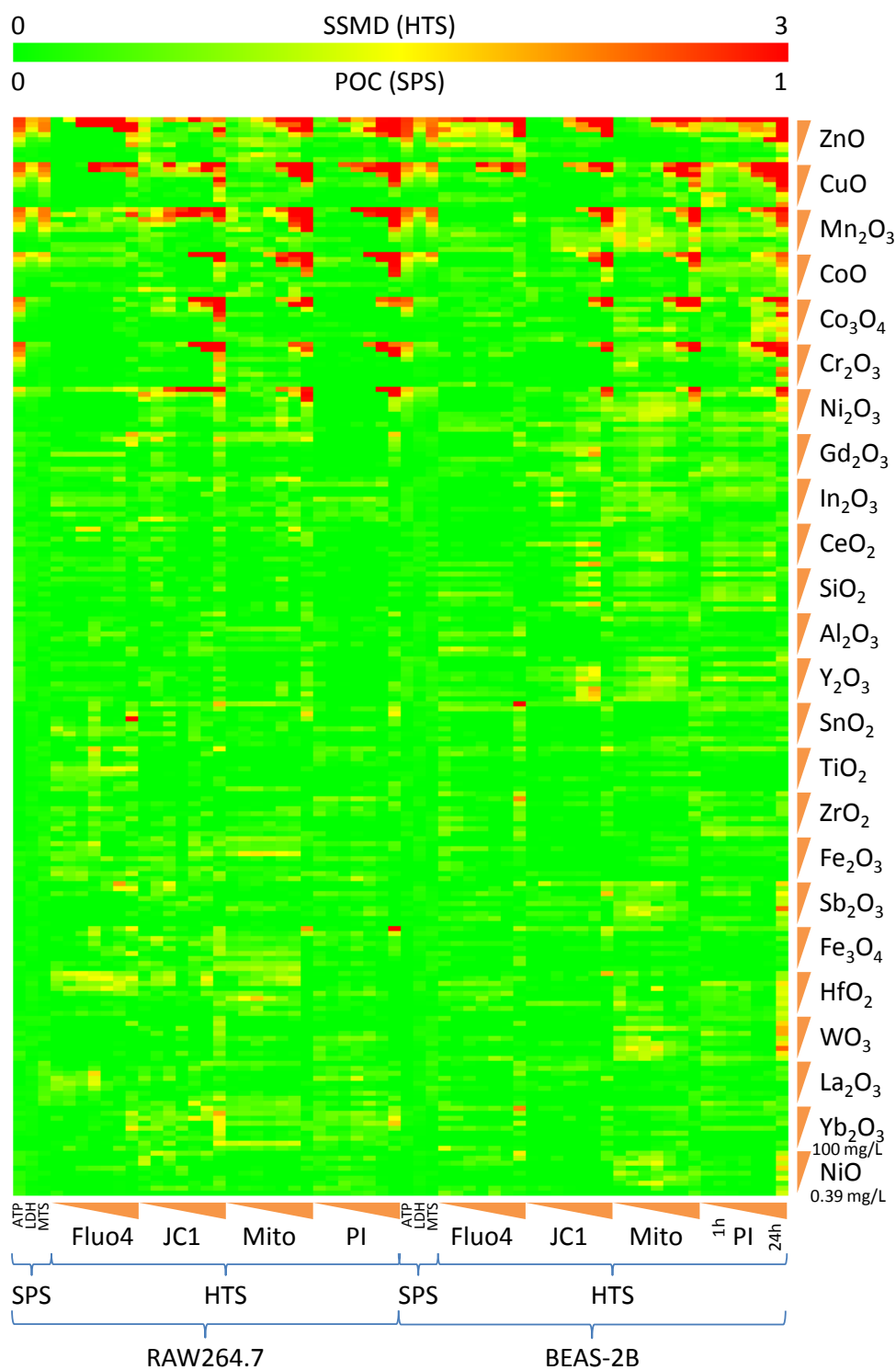


Figure S1. Toxicity of the NPs (exposure concentration: 0.39-100 mg/L, exposure time: 1-24h). SPS data were normalized as percent of control (POC) and the HTS data were normalized using the strictly standardized mean difference (SSMD). Higher POC/SSMD values indicate greater level of toxicity.

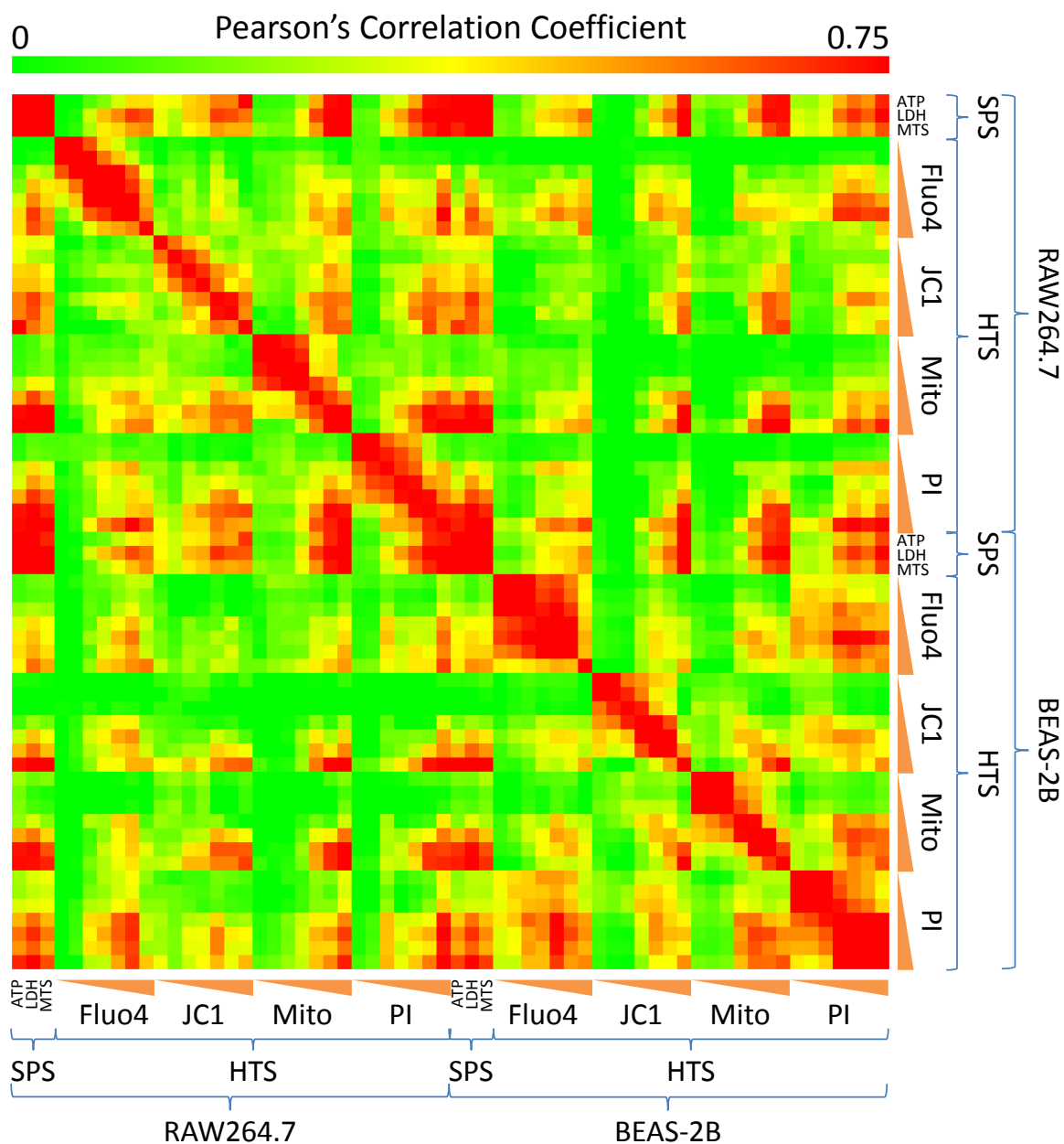


Figure S2. Pearson Correlation between different toxicity assays. A Pearson correlation coefficient (r) indicates a moderate positive linear correlation for $r \sim 0.38-0.75$ and a strong positive linear correlation²² for $r > 0.75$.

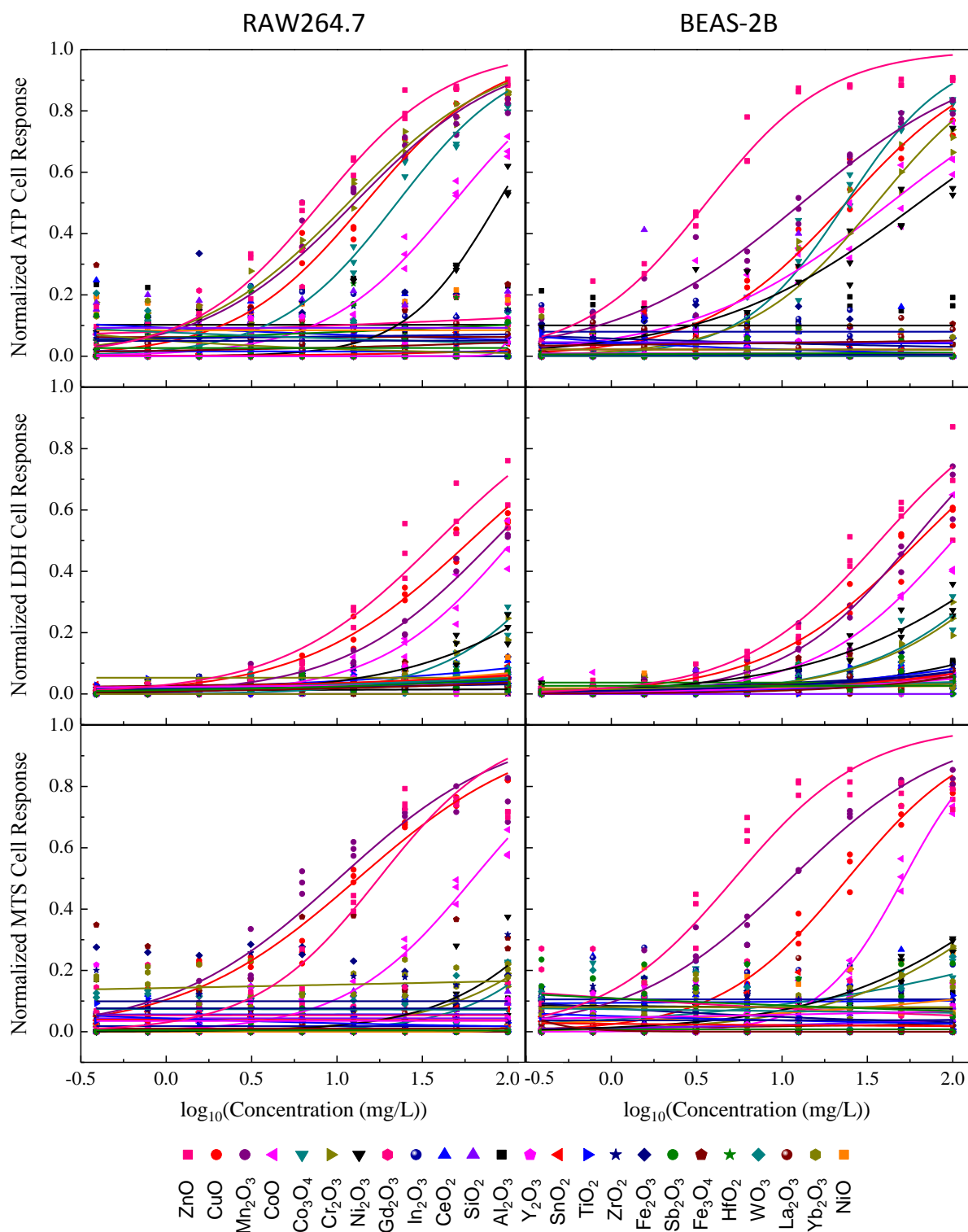


Figure S3. Dose-Response curves fitted to the SPS data (ATP, LDH, and MTS assays). A log-logistic function ($y = 1/(1 + 10^{s(\log_{10}EC50 - \log_{10}x)})$) was fitted to the NP induced cell responses (in triplicate) at each concentration (x). The ZnO, CuO, Mn₂O₃, CoO, Co₃O₄, Cr₂O₃, and Ni₂O₃ NPs show clear dose-response behavior.

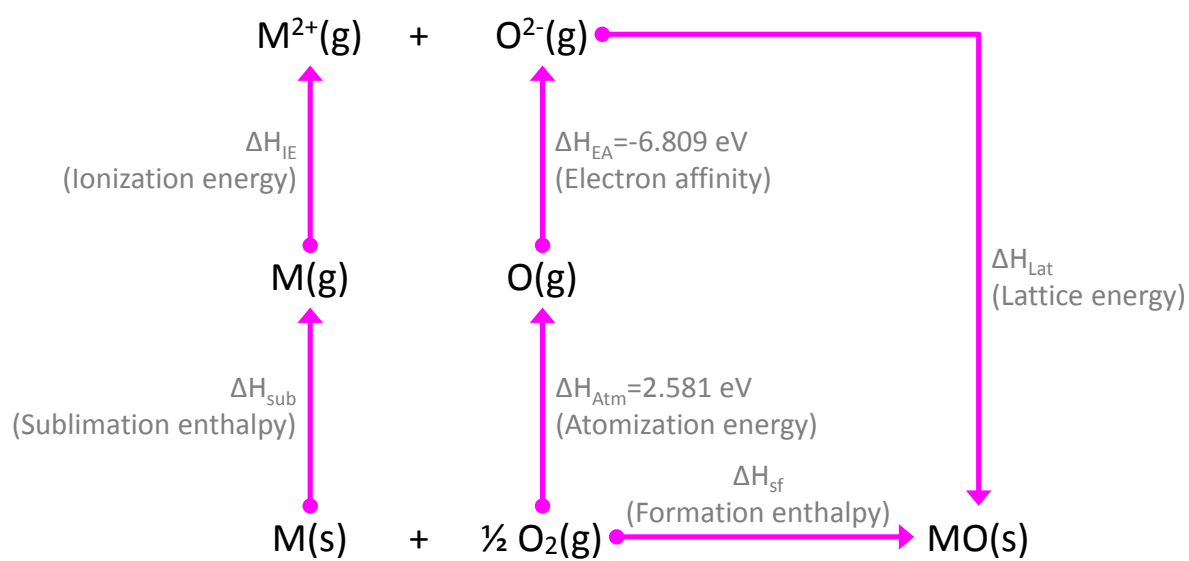


Figure S4. An illustration of Born-Haber Cycle³⁵ for metal oxide (MO). The symbols “s” and “g” identify solid and gas phases, respectively.

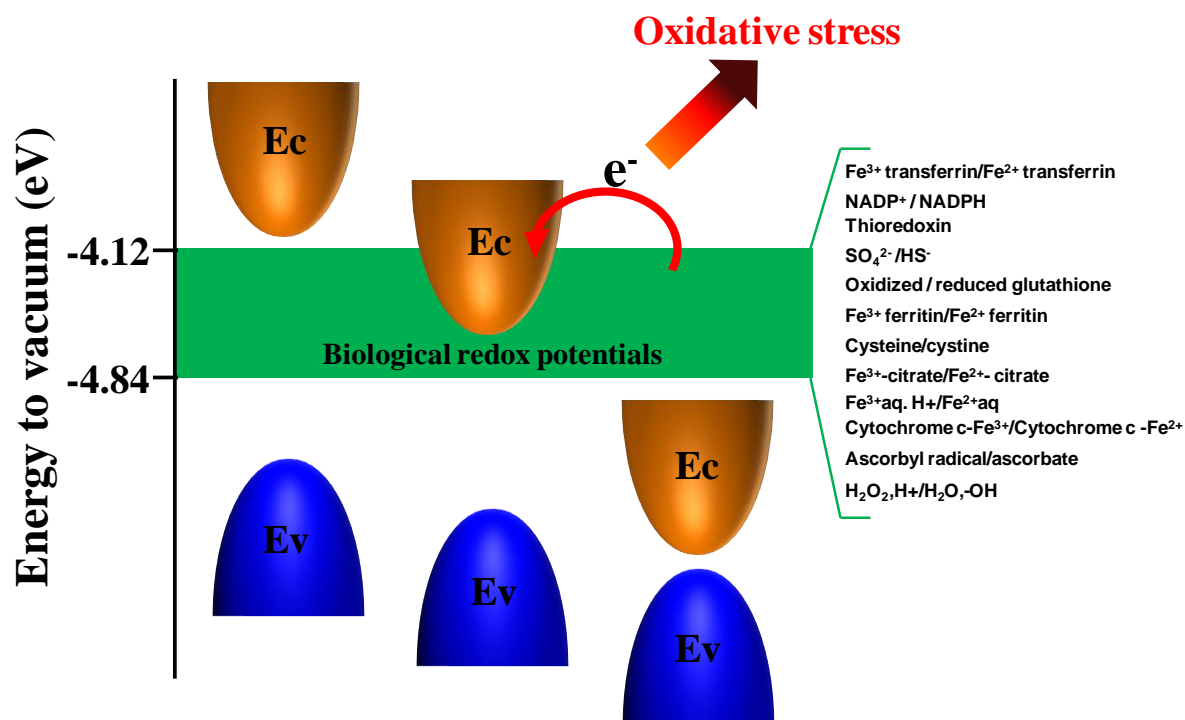


Figure S5. Conduction band energy as a factor of cellular oxidative stress generation. Electron transfer from biological material to NP might occur and lead to cellular oxidative stress generation if the NP's conduction band energy is within [-4.84, -4.12] eV (an estimated standard redox potentials of couples active in biological media with respect to the absolute vacuum scale)³⁶.

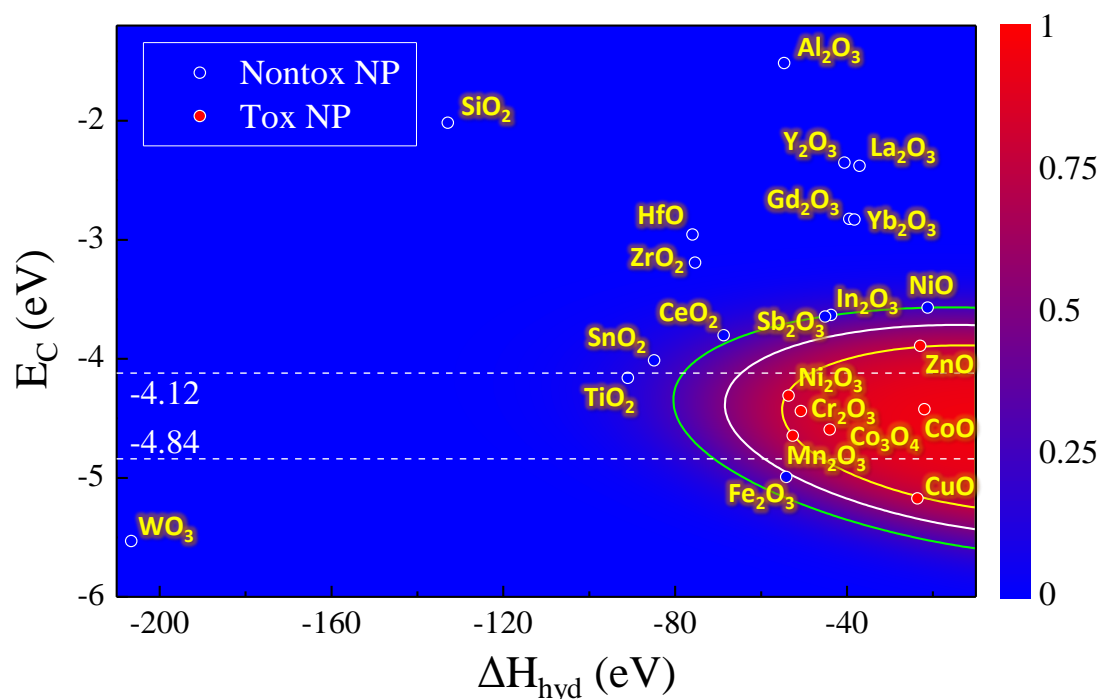


Figure S6. Toxicity probability of NP (x) belonging to the toxic class (T) given by the SVM based nano-SAR using conduction band energy (E_C) and hydration enthalpy (ΔH_{hyd}). The posterior toxicity probability $P(T|x)$ is depicted via the color map in the descriptor space. The middle contour, which is for $P(T|x)=0.5$, defines the nano-SAR classification boundary, while the inner ($P(T|x)=0.73$) and outer ($P(T|x)=0.27$) contours correspond to the decision boundaries for penalty ratios of false negative relative to false positive predictions (i.e., $L_{\text{FN}}:L_{\text{FP}}$) set as 1:2.7 and 2.7:1, respectively. The hydration enthalpy (ΔH_{hyd}) was estimated via Latimer's equation^a ($\Delta H_{\text{hyd}}=-631.184Z^2/(r+50)$ eV). The nano-SAR classification accuracy was 93.2%. Note: For nano-SAR developed using a mix of reported experimental hydration enthalpy^b values along with calculated values for those lacking experimental data (i.e., Co_3O_4 , Ni_2O_3 , Sb_2O_3 , SiO_2 , TiO_2 , and WO_3), the classification accuracy is found to decrease to 90.2%.

^a Wulfsberg, G. *Principles of descriptive inorganic chemistry*. (University Science Books, 1991).

^b Smith, D. Ionic hydration Enthalpies. *Journal of Chemical Education* **54**, 540-542 (1977).

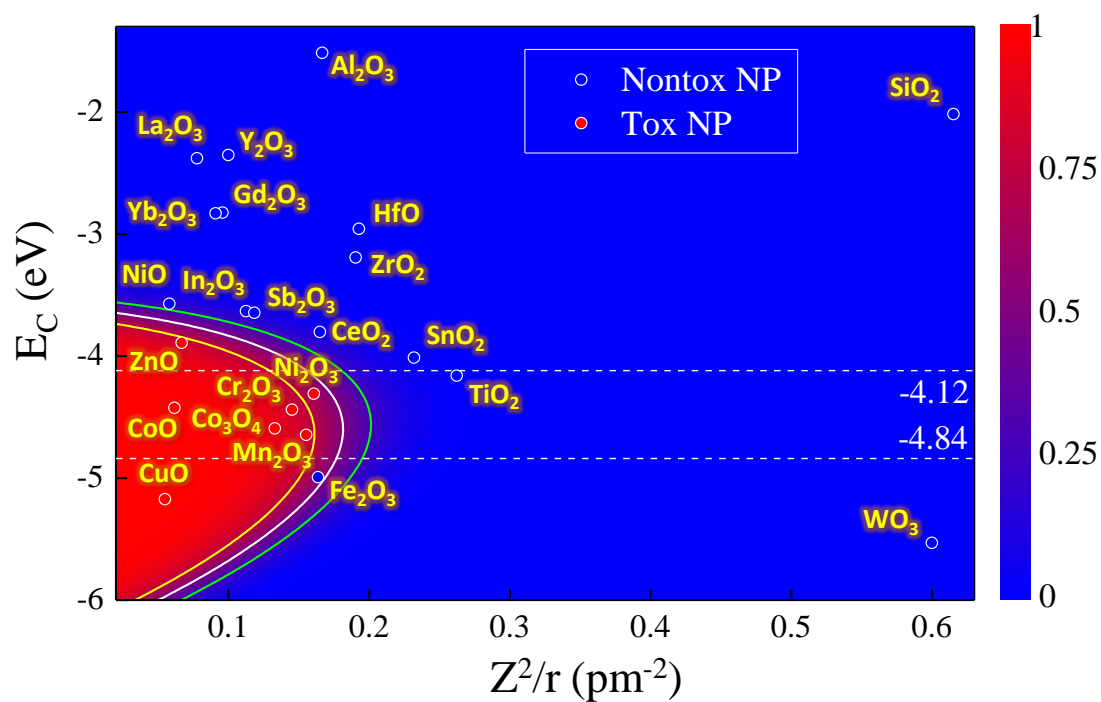


Figure S7. Toxicity probability of NP (\mathbf{x}) belonging to the toxic class (T) given by the qLGR based nano-SAR. The posterior toxicity probability $P(T|\mathbf{x})$ is depicted in the color map in the descriptor space. The middle contour for which $P(T|\mathbf{x})=0.5$ defines the nano-SAR classification boundary, while the inner ($P(T|\mathbf{x})=0.73$) and outer ($P(T|\mathbf{x})=0.27$) contours correspond to the decision boundaries for penalty ratios of false negative relative to false positive predictions (i.e., $L_{FN}:L_{FP}$) set as 1:2.7 and 2.7:1, respectively.

Table S1. Descriptors (physicochemical properties) of the nanoparticles^{a,b}

| NP | dp | E_C | E_V | E_{Amz} | χ_{MeO} | ΔH_{sub} | ΔH_{IE} | ΔH_{sf} | ΔH_{Lat} | $\Delta H_{IE,1+}$ | Z^2/r | IEP | ZP |
|--------------------------------|--------------|--------|---------|-----------|--------------|------------------|-----------------|-----------------|------------------|--------------------|-----------|------|-------|
| | nm | | | | | | | | | | pm^{-2} | pH | mV |
| ZnO | 22.6 ± 5.1 | -3.891 | -7.198 | 7.546 | 5.674 | 1.351 | 28.710 | -3.608 | 42.928 | 9.394 | 0.0667 | 9.6 | 28.8 |
| CuO | 12.8 ± 3.4 | -5.174 | -6.515 | 7.719 | 5.874 | 3.497 | 31.515 | -1.609 | 42.856 | 7.726 | 0.0548 | 7.9 | 7.6 |
| Mn ₂ O ₃ | 51.5 ± 7.3 | -4.647 | -7.635 | 11.709 | 5.919 | 2.936 | 59.677 | -9.917 | 156.975 | 7.434 | 0.1552 | 3.7 | -46.1 |
| CoO | 71.8 ± 16.2 | -4.424 | -6.832 | 9.454 | 5.735 | 4.422 | 29.387 | -2.476 | 39.767 | 7.881 | 0.0615 | 9.2 | 21.6 |
| Co ₃ O ₄ | 10.0 ± 2.4 | -4.593 | -7.025 | 10.755 | 5.927 | 4.422 | 46.137 | -9.380 | 99.573 | 7.881 | 0.1329 | 9.4 | 24.6 |
| Cr ₂ O ₃ | 193.0 ± 90.0 | -4.439 | -7.524 | 13.920 | 5.858 | 4.120 | 58.331 | -11.717 | 158.322 | 6.767 | 0.1452 | 5.3 | -32.6 |
| Ni ₂ O ₃ | 140.6 ± 52.5 | -4.309 | -7.688 | 11.709 | 6.052 | 4.458 | 65.455 | -5.073 | 164.157 | 7.639 | 0.1607 | 8.3 | 32.2 |
| Gd ₂ O ₃ | 43.8 ± 15.8 | -2.825 | -8.102 | 16.782 | 5.499 | 4.120 | 42.989 | -18.820 | 134.692 | 6.150 | 0.0957 | 8.0 | 6.5 |
| In ₂ O ₃ | 59.6 ± 19 | -3.632 | -7.322 | 11.188 | 5.583 | 2.518 | 55.204 | -9.606 | 144.351 | 5.786 | 0.1125 | 9.2 | 61.9 |
| CeO ₂ | 18.3 ± 6.8 | -3.803 | -7.450 | 20.121 | 5.650 | 4.354 | 77.697 | -11.284 | 99.775 | 5.539 | 0.1649 | 7.8 | 21.4 |
| SiO ₂ | 13.5 ± 4.2 | -2.018 | -11.118 | 18.734 | 6.190 | 4.664 | 107.795 | -9.410 | 136.029 | 8.151 | 0.6154 | 1.0 | -31.8 |
| Al ₂ O ₃ | 14.7 ± 5.2 | -1.515 | -9.815 | 15.872 | 5.665 | 3.429 | 56.691 | -17.345 | 164.955 | 5.985 | 0.1667 | 7.4 | 0.0 |
| Y ₂ O ₃ | 32.7 ± 8.1 | -2.352 | -8.201 | 17.433 | 5.406 | 4.402 | 43.362 | -19.748 | 131.676 | 6.217 | 0.1000 | 9.6 | 42.7 |
| SnO ₂ | 62.4 ± 13.2 | -4.013 | -8.013 | 14.397 | 5.812 | 3.122 | 96.334 | -5.986 | 122.369 | 7.344 | 0.2319 | 4.0 | -38.8 |
| TiO ₂ | 12.6 ± 4.3 | -4.161 | -7.491 | 19.775 | 5.767 | 4.902 | 96.063 | -9.779 | 125.924 | 6.828 | 0.2623 | 6.4 | -19.4 |
| ZrO ₂ | 40.1 ± 12.6 | -3.192 | -8.233 | 22.723 | 5.618 | 6.322 | 83.379 | -11.252 | 115.954 | 6.634 | 0.1905 | 5.8 | -12.8 |
| Fe ₂ O ₃ | 12.3 ± 2.9 | -4.993 | -6.987 | 12.489 | 5.978 | 4.306 | 59.047 | -8.512 | 148.300 | 7.903 | 0.1636 | 7.2 | -2.1 |
| Sb ₂ O ₃ | 11.8 ± 3.3 | -3.645 | -8.138 | 10.408 | 5.514 | 2.740 | 53.278 | -7.346 | 142.071 | 8.608 | 0.1184 | 1.0 | -35.3 |
| HfO ₂ | 28.4 ± 7.3 | -2.956 | -8.371 | 23.938 | 5.705 | 6.409 | 84.863 | -1.170 | 104.812 | 6.825 | 0.1928 | 8.1 | 33.5 |
| WO ₃ | 16.6 ± 4.3 | -5.532 | -8.586 | 24.978 | 6.640 | 8.820 | 213.421 | -8.734 | 250.324 | 7.864 | 0.6000 | 0.3 | -61.3 |
| Yb ₂ O ₃ | 61.7 ± 11.3 | -2.831 | -7.933 | 15.091 | 5.429 | 1.613 | 45.092 | -18.807 | 138.672 | 6.254 | 0.0909 | 8.2 | 9.9 |
| La ₂ O ₃ | 24.6 ± 5.3 | -2.380 | -8.147 | 17.433 | 5.378 | 4.467 | 40.280 | -18.668 | 129.054 | 5.577 | 0.0776 | 9.4 | 54.3 |
| NiO | 13.1 ± 5.9 | -3.570 | -7.445 | 9.454 | 5.744 | 4.458 | 30.266 | -2.494 | 40.503 | 7.639 | 0.0580 | 11.4 | 27.6 |

^a d_p : primary nanoparticle (NP) size (given in the format of average size (d) ± standard deviation (σ)), E_C : NP energy of conduction

band, E_V : NP energy of valence band, E_{Amz} : metal oxide atomization energy, χ_{MeO} : metal oxide electronegativity, ΔH_{sub} : metal oxide

sublimation enthalpy, ΔH_{IE} : metal oxide ionization energy, ΔH_{sf} : metal oxide standard molar enthalpy of formation, ΔH_{Lat} : metal oxide lattice enthalpy, $\Delta H_{IE,1+}$: first molar ionization energy of metal, Z^2/r : ionic index of metal cation; IEP: NP isoelectric point, ZP: NP zeta potential in water at PH of 7.4; E_{Amz} was converted from the atomization energy in kcal/eqv. The atomization energy of Ni_2O_3 is lacking and thus was estimated as that of Mn_2O_3 since they share the same molecular structure and the atomization energies of NiO and MnO are identical. Note that the enthalpies involved in Born-Haber cycle for Co_3O_4 were calculated by taking the average of those for CoO and Co_2O_3 . Also, the Ionic index of the metal ion in Co_3O_4 was estimated as the weighted average (1:2) of Co^{2+} and Co^{3+} in the metal oxide NP crystal.

^bThirty descriptors were used for nano-SAR development. Fourteen of the descriptor values are provided in the Table, while the remaining 16 can be easily calculated as described below.

- i. Seven descriptors based on primary NP size were evaluated for SAR development, including: different orders of average size (d^2 , d^1 , d , d^2), standard deviation (σ), mean/standard deviation ratio (d/σ), and coefficient of variation (σ/d);
 - ii. Three other quantum mechanics descriptors were derived from E_C and E_V , including chemical potential ($\mu=(E_C+E_V)/2$), chemical hardness ($\eta=(E_C-E_V)/2$), and electrophilicity ($\omega=\mu^2/2\eta$);
 - iii. Fundamental metal oxide descriptors were also included in the initial pool of descriptor, including numbers of metal and oxygen atoms, atomic mass of metal and metal oxide molecular weight, group and period of metal (in periodic table), and electronegativity of metal; these are not listed in the above table as they can be easily ascertained from the metal oxide chemical formula.
-